Perspective

Reconsidering the Benchmarking Evaluation of Catalytic Activity in Oxygen Reduction Reaction

Wenlong Chen,[1,3] Qian Xiang,[1,3] Tao Peng,[1] Chengyi Song,[1] Wen Shang,[1] Tao Deng,[1,2] and Jianbo Wu[1,2,4,*]

The sluggish kinetics of the oxygen reduction reaction (ORR) on electrocatalysts represents a major obstacle in the development of fuel cell technology. A tremendous amount of work has reported the increasing ORR activity for catalysts. Nevertheless, when applied to practical Membrane Electrode Assembly (MEA, an assembled stack of a proton exchange membrane fuel cell) configuration, the high-performance catalysts on the rotating disk electrode (RDE) may not display the same high activity as in the lab-scale tests. This led us to reexamine the ORR evaluation based on the RDE technique. With the development of high active electrocatalysts, it may become significant to determine the reasonable kinetic current at a conventional fixed potential approaching the limited current by using the Koutecky-Levich (K-L) technique on RDE for the evaluation of ORR activity. Here we describe such a challenging situation and systematically discuss the proper kinetic region when comparing the ORR activity with the unsuitable potential or Pt loading based on the K-L technique. Furthermore, the rational benchmarking guidelines are given for the evaluation of the ORR electrocatalysts.

INTRODUCTION

With the onset of great challenges such as environmental change and the scarcity of traditional fuels now, electrocatalysts functioning within energy storage and conversion devices have been rapidly developed. Such devices are being developed currently because they have the capacity to use low-cost electricity potentially from renewables to meet energy needs. Proton exchange membrane fuel cells (PEM-FCs) are a vital part of this growth and future of renewable energy applications. The sluggish kinetics of the oxygen reduction reaction (ORR), one of the half-reactions that makes up the whole fuel cell process, on electrocatalysts represents a major obstacle to a more widespread use not only for fuel cells but also for metal-air batteries. Developing and optimizing highly active catalysts has become paramount for the optimization of fuel cell performance. For highly active ORR electrocatalysts, the activation energy barriers should be low in its reaction kinetics steps, and the specific and mass current activity in the electrochemical process should be observed as high as possible in certain overpotentials when compared with other catalysts. Parameters such as these are common figures of metric within this field to understand activity and benchmarking catalysts.

From previous studies, the mass activity of a commercial TKK Pt/C catalyst is around $0.28 \, mA \, \mu g_{Pt}^{-1}$ at 0.9 V versus RHE (Pedersen et al., 2015). Thanks to the efforts of different studies, more high-performance ORR catalysts have been explored in recent years. Various efficient strategies have been applied to obtain highly acitive catalysts (Wu and Yang, 2013, Liu et al., 2019), such as surface engineering to fabricate a 3D hollow PtNi structure with open Pt-skin framework (Chen et al., 2014) and hollow PtNi cages (Tian et al., 2019), doping method to synthesize Mo-doped Pt_3Ni (Huang et al., 2015), 1D jagged Pt nanowires (Li et al., 2016), 2D PtPb/Pt nanoplates with biaxial strain (Bu et al., 2016). With these strategies, the ORR mass activity could achieve to $\sim13 \, A \, mg_{Pt}^{-1}$ (Liu et al., 2019). However, few catalysts with extraordinary activities have been perfectly introduced into the full fuel cell configuration yet. There still is a tremendous gap between the reported performance indicated by RDE results and practical performance studied in MEA. Further studies are warmly expected to meet the practical application of advanced catalysts in such devices.

Nevertheless, as the potential development of active electrocatalysts with increasing performance, the conventional results obtained at 0.9 V may become not reasonable in the case of a rational benchmark (Stephens et al., 2016). It may become challenging to rationally determine the reasonable kinetic current by using the RDE

[1]State Key Laboratory of Metal Matrix Composites, School of Materials Science and Engineering, Shanghai Jiao Tong University, 200240 Shanghai, China

[2]Center of Hydrogen Science, Shanghai Jiao Tong University, 200240 Shanghai, China

[3]These authors contributed equally

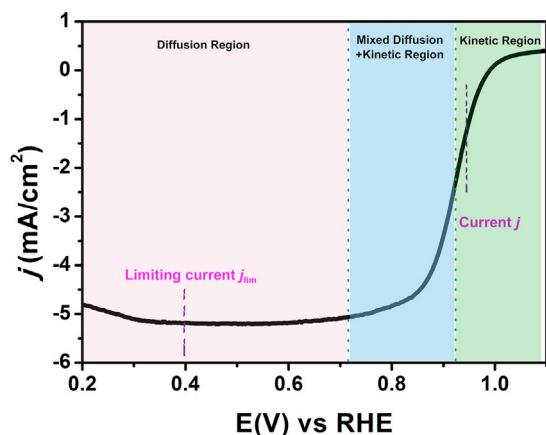[4]Lead Contact

*Correspondence: jianbowu@sjtu.edu.cn

Figure 1. The Different Oxygen Reduction Regions in a Typical RDE LSV Curve

The different oxygen reduction regions in a typical RDE LSV curve for a rotating Pt electrode in an acidic electrolyte saturated with oxygen that is characteristic of kinetic and mass transport limiting processes.

method technique for the evaluation of ORR activity toward the materials with extremely high ORR activity because the kinetic current value obtained from the K-L method (Zhou et al., 2016) under the overpotential approaching the limited diffusion current becomes inaccurate for the calculation of the specific and mass activities (e.g. 0.9 V vs. RHE, which is usually considered the benchmark potential for ORR catalysts).

For the O_2 concentration in the electrolyte (C_e), the actual O_2 concentration at the electrode surface (C_s) is lower than C_e due to the consumption of O_2 as a function of current density. The K-L equation is conventionally applied to account for this difference in concentration so that i_k at C_e is obtainable. However, it is essential to note that the evaluation of the real kinetic current based on the K-L method is conditional and is therefore dependent on many corrections.

The data analysis and evaluation of electrocatalysts for ORR is usually based on the ORR polarization curves, which generally would display three regions among the whole potential range, that is, the kinetic control region, kinetic-diffusion mixed control region, and the diffusion limiting region (Figure 1). The so-called K-L plots are often used as a standard approach to evaluate the kinetic current in order to present and compare the activities of catalysts at 0.9 V practically (Pasti et al., 2012; Gasteiger et al., 2005). Nowadays, a large amount of explored electrocatalysts have approached the diffusion-limited region with much lower overpotential (Liu et al., 2019; Li et al., 2019; Shao et al., 2016). In regard to this situation, some of the studies emphasized the activity at 0.95 V versus RHE (Huang et al., 2015; Liu et al., 2019). With the fast development of highly active electrocatalysts, the evaluation of kinetic activity in some higher overpotentials hence may lead to a magnified inaccuracy. In such situation, the results estimated through the polarization curves include the effect of mass transfer, and the values obtained from the K-L equation are not able to reveal the real activity of the catalysts anymore and not reliable to compare with other catalysts. With the development of the advanced ORR catalysts, an unambiguous activity benchmark is a prerequisite to make sense and to prove the intrinsic high activity (but not just the value obtained from the mathematical equation without the consideration of conditions) of the materials for fuel cells. In this work, we systematically illustrated and discussed the proper kinetic region when comparing the ORR activity under large overpotential based on the K-L technique, and subsequently, rationalize benchmarking guidelines for the measurement and evaluation of catalysts studied using for the RDE method.

RESULTS

To illustrate the aforementioned issues and demonstrate the unreasonable and contradictory evaluation of the ORR catalysts when the overpotential goes beyond the kinetic potential region and approaches to the diffusion-limited region, firstly, we studied the activities of the commercial Pt/C catalyst at different potentials, as it is the widely used benchmark catalyst in fuel cell (Figure 2).

We designed an experiment with a series of different mass loadings of the commercial Pt/C on the RDE (see Transparent Methods for details) to demonstrate the difference for the evaluation of catalyst activity when calculating the kinetic current (j_k) (Figure 2). Figure 2A shows that the electrochemical surface active areas (ECSAs) are obtained from the hydrogen adsorption region (0.05–0.4 V versus RHE). The ECSAs are
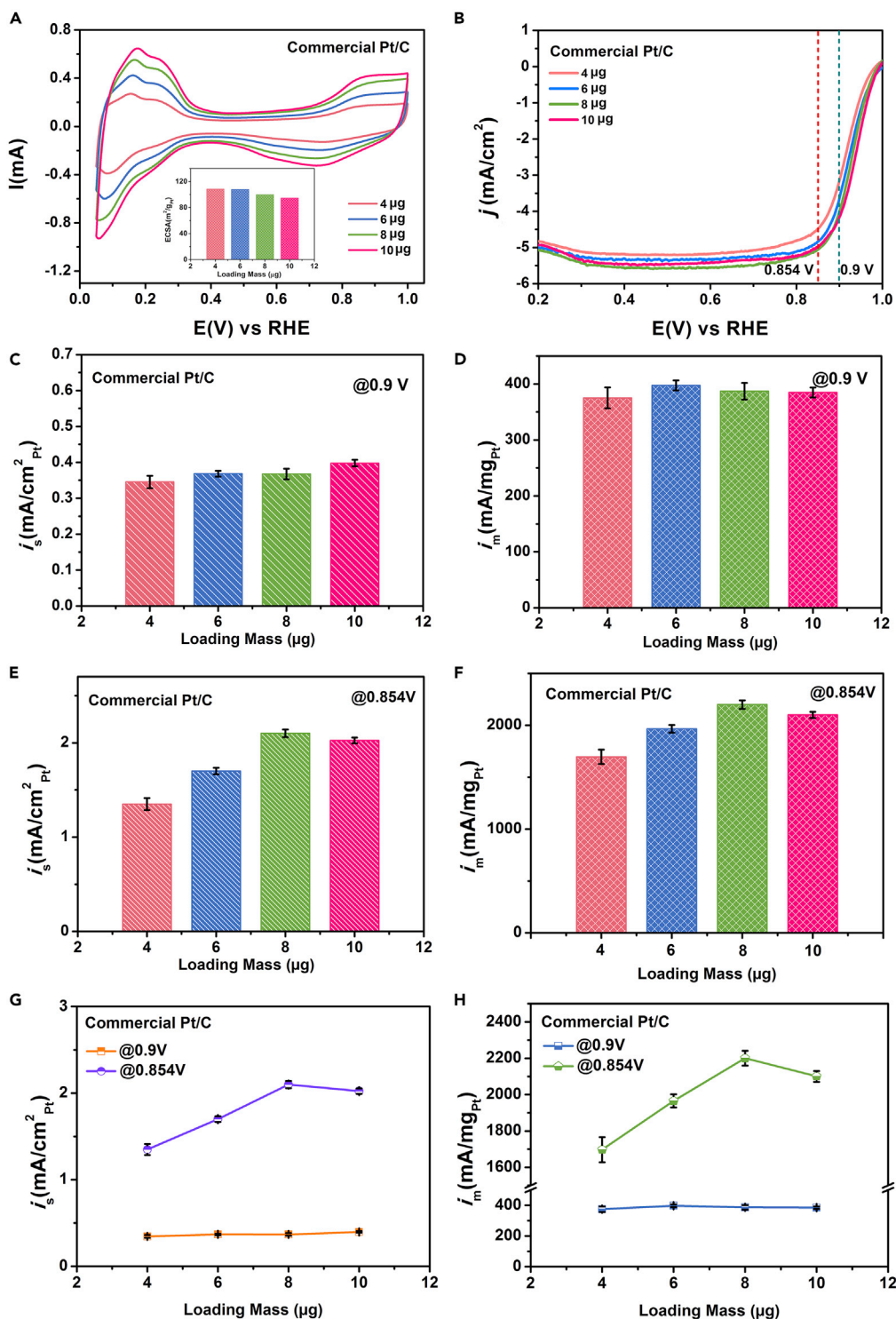
Figure 2. ORR Performance of the Commercial Pt/C at 0.9 V and 0.854 V with Different Mass Loadings.

(A) CV curves of the commercial Pt/C with different mass loadings.

(B) ORR polarization curves for commercial Pt/C with iR-drop correction.

(C and D) (C) Specific and (D) mass ORR activities for commercial Pt/C catalysts at the potential of 0.9 V versus RHE.

Figure 2. *Continued*

(E and F) (E) Specific and (F) mass ORR activities for commercial Pt/C catalyst with various mass loading at the potential of 0.854 V versus RHE

(G and H) Comparison of (G) specific and (H) mass ORR activities of the catalysts at different potentials as 0.854 V and 0.9 V versus RHE. Error bars represent one standard deviation of multiple independent measurements.

108.5, 107.92, 99.8, and 94.6 m^2/g_{Pt}, as increasing the mass loading from 4 μg to 6, 8, and 10 μg, respectively. The slight decrease of the ECSA for 8–10 μg catalysts is due to the lack of full utilization of active sites in the thick catalyst layer. Figure 2B illustrated the ORR LSV curves measured for all the Pt/C with different mass loadings based on the RDE after *i*R correction (see Transparent Methods for details). The area-specific and mass activities for ORR were calculated based on the ORR curves by normalizing the kinetic current density (i_k) to the above ECSA and the mass loading amount of Pt/C, respectively (Figures 2C–2D). The results of the specific (i_s) and mass (i_m) activities demonstrated that the activities changed in volcanic plots as the increase of catalyst loadings, whereas the 6 μg loading RDE reached the highest i_m of 0.397 mA/$μg_{Pt}$. It should be noted that, although different, the i_m ranging from 4 to 10 μg was similar (0.375, 0.398, 0.385, 0.384 mA/$μg_{Pt}$). In this case, the loading of Pt/C is not sensitive to determine the performance at 0.9 V.

Figure 2B also shows the more loading of Pt has a smaller overpotential to reach the diffusion-limited current (j_{lim}). In order to describe the magnified inaccuracy and the rising error of the evaluation of ORR catalysts in the larger overpotential position for different Pt loading, we calculated ORR activities at 0.854 V (Figures 2E and 2F). At 0.854 V, both sequences of the i_s and i_m values vary more dramatically (30% deviation) among the different loadings compared with those at 0.9 V (5.6% deviation) (Figures 2H and 2G). It can be expected that, with the potential chosen more close to the diffusion-limited region, the relative error and deviation of the calculated activities would dramatically grow larger. Obviously, it revealed that unsuitable choice of mass loading to evaluate the ORR activities may induce misleading of the real performance of catalysts. Consequently, the above discussion indicated that even for the same catalyst with different mass loading on the RDEs, the mass and specific activities can be significantly different at a given potential.

Why could the potential of 0.9 V be used reasonably for all the four RDEs while the 0.854 V seemed unreliable to calculate the kinetic current for ORR correctly, and how shall we determine the rational potential as a benchmarking? Here, we used Tafel plots to explain this phenomenon and determination of the inappropriate value.

The electrokinetic Tafel equation (Holewinski and Linic, 2012):

$$\Delta E = a + b \log(i)$$

Here, δE represents the difference of potential between the equilibrium potential and the applied potential, whereas *a* represents a constant that is related to the current at the equilibrium. What is more, *b* is the Tafel slope. Thus, the Tafel equation could give a linear relation between the logarithm of current and electrode potential (Damjanovic and Sepa, 1990). Nevertheless, it has been widely and experimentally reported that the Tafel slope changes a lot with the applied potential for many electrocatalytic reactions, including the ORR on Pt, as the reaction orders have also been demonstrated to vary with different potential (Blizanac et al., 2006; Gasteiger et al., 2005). Previous research revealed that the measured Tafel slopes shift from ∼60 mV/dec (at small overpotential) to ∼120 mV/dec (at larger overpotential) for the ORR on Pt (Holewinski and Linic, 2012; Gasteiger et al., 2005). And it is in agreement with the initial electron transfer as the sole rate-limiting step (RLS) during the whole reaction range of operating potentials (Damjanovic and Sepa, 1990; Wang et al., 2007; Marković et al., 1999, 2001). Thus, it is found that the ORR Tafel slope of 120 mV/dec indicates the initial electron transfer to O_2. Moreover, the region of the Tafel slope between 60 and 120 mV/dec also suggests a mechanism that is limited by the initial reduction of O_2 (Walsh et al., 2013). We believe that the appropriate value to calculate the kinetic current should be in the kinetic-limited region where the Tafel slope was less than 120 mV/dec.

The Tafel plots of the commercial Pt/C catalyst with different potentials derived from the ORR polarization curves were adopted to find out the proper overpotential range that could be used to calculate the "real" kinetic current (Figures 3A–3D). From curves, the potentials at the Tafel slope of 120 mV/dec for different Pt/C loadings were derived to 0.851 V, 0.854 V, 0.861 V, and 0.863 V from 4 to 10 μg,
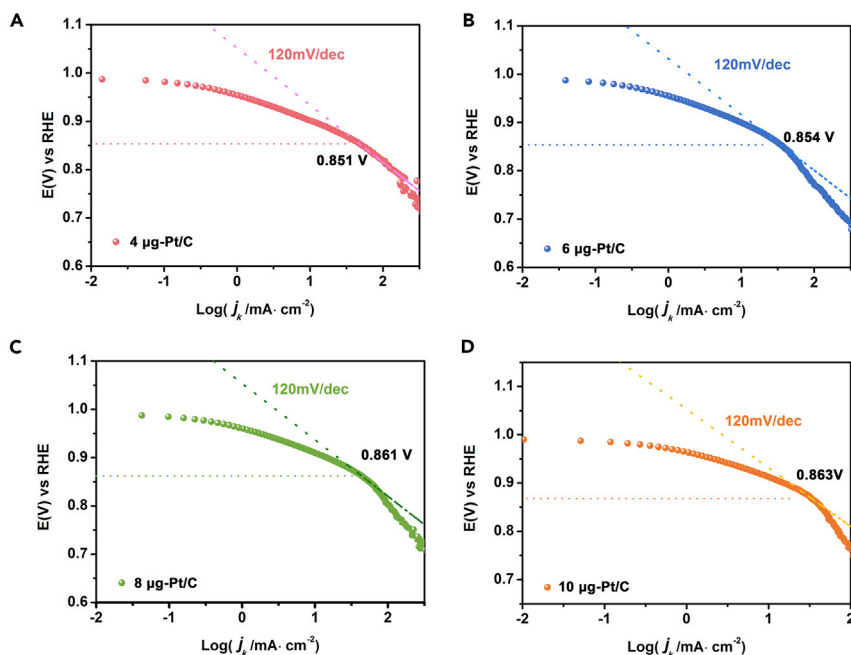
Figure 3. Tafel Plots of the Commercial Pt/C Catalyst with Different Potentials Derived from the ORR Polarization Curves

(A–D) Tafel plot for the commercial Pt/C catalyst with the mass loading of (A) 4 μg, (B) 6 μg, (C) 8 μg, and (D) 10 μg; the measurements are tested in O_2-saturated 0.1M $HClO_4$ electrolyte.

respectively. As mentioned earlier, the calculation of the i_k at the potential of 0.9 V versus RHE (Figure 2) is in a kinetic-controlled region with a Tafel slope lower than 120 mV/dec. Thus, at 0.9 V, the specific and mass activities for commercial Pt/C are reasonable for all the different loadings. Instead, when using 0.854 V to determine the activity, it was still nearly fair for the 4 μg and 6 μg loadings. However, the 8 μg and 10 μg Pt loadings make the reaction beyond the kinetic current region because the Tafel slopes are larger than 120 mV/dec for these two cases (Figures 3C and 3D). Figure 3 shows the slope at 0.854 V is in the region where the diffusion effect could not be neglected (the Tafel slope is higher than 120 mV/dec) for the different Pt/C loadings. Under this condition, the current at the potentials smaller than 0.854 V will gradually approach the value of limiting current, and the kinetic current will approach infinity in theory according to the K-L equation. Therefore, the 0.854 V is not suitable as the benchmark to evaluate the kinetics current for the higher Pt loading RDEs (8 μg and 10 μg) but can still nearly fair for the 4 μg and 6 μg ones (Note: in this situation, the potential is still near the critical value, which may still have relative inaccuracy to some extent to evaluate the ORR activity). Based on the above discussion, we can conclude that when evaluating the kinetic current at the given potentials (e.g. 0.9 V), a suitable catalyst loading should be carefully considered to ensure the reaction is in the kinetics region with Tafel slops smaller than 120 mV/dec.

As mentioned earlier, we have demonstrated the proper loading to evaluate the real activity using the commercial Pt/C catalyst as an example. In order to further prove this protocol applicable for the practical highly active catalysts, we also test out the ORR performance for Pt_3Ni/C catalysts with the Pt loading of 3 μg, 3.5 μg, and 6 μg on RDE (Figure 4A), as the Pt-Ni catalysts have been widely reported with superior ORR activities among the advanced Pt-based nanomaterials (Wu and Yang, 2013; Wu et al., 2010, Wu et al., 2011, Wu et al., 2012). Figure 4D shows that the critical Tafel slope value of 120 mV/dec is at 0.910 V for the 6 μg Pt loading, which means the ORR kinetics current at 0.9V potential would cause inaccuracy and error using K-L equation and it could not be used to fairly compare with other catalysts. However, we can make the 0.9 V position in the kinetic-control region to calculate kinetic current by reducing the catalyst loading. Hence, when we reduce the Pt loading to 3 μg and 3.5 μg, as a result, the position of the critical Tafel slope value of 120 mV/dec shift to 0.873 V and 0.884 V, respectively (Figures 4B and 4C), which would allow the accuracy to evaluate the ORR activity at 0.9 V. As expected, the mass activity of the 3 μg and 3.5 μg Pt loading catalysts showed the similar fair value of ~2.3 mA/μg$_{Pt}$ with a variation of 4.5%. However, the
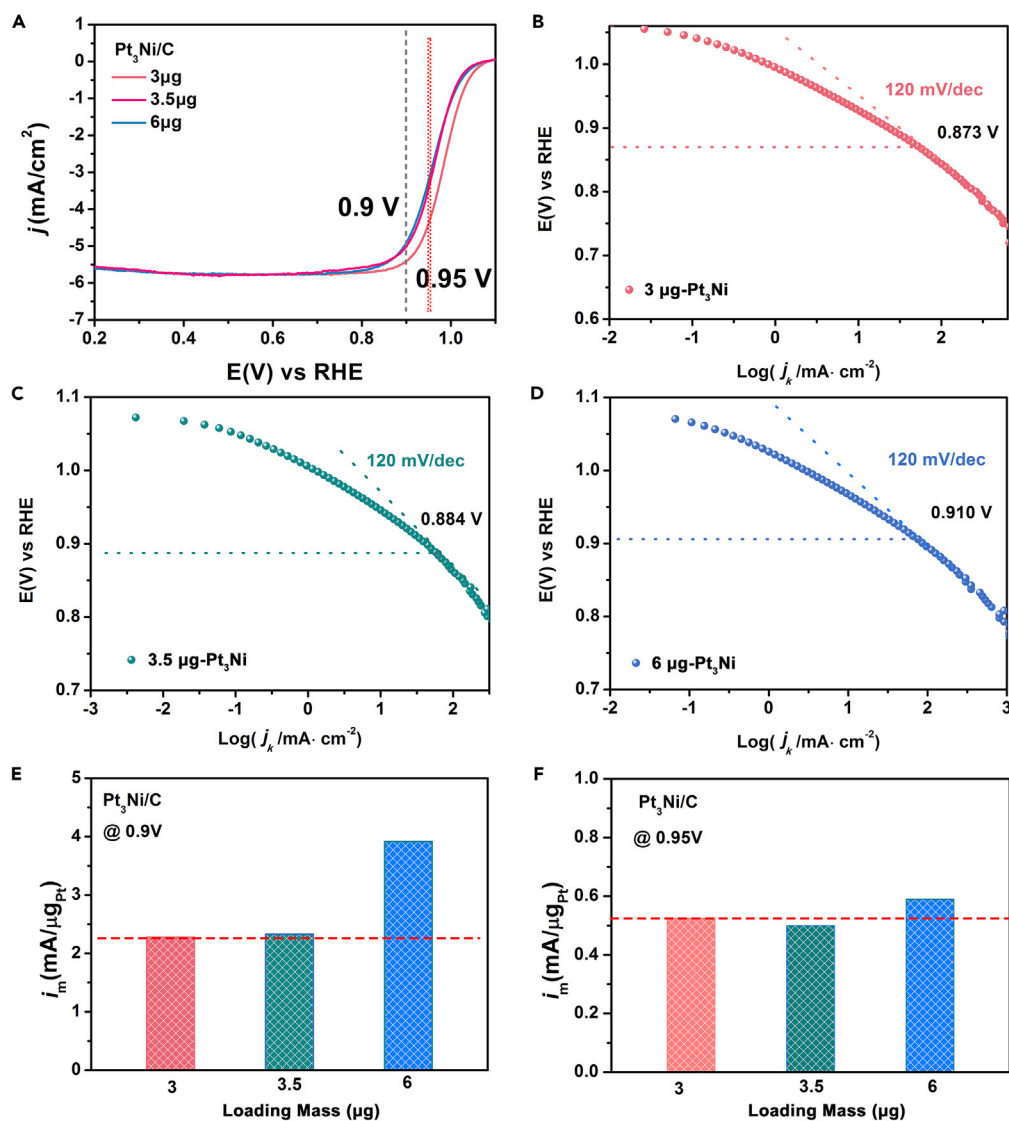
Figure 4. ORR Performance of the Pt₃Ni/C Catalyst in 0.1M HClO₄

(A–F) (A) ORR polarization curves for Pt₃Ni/C with iR-drop correction. Tafel plot for the Pt₃Ni/C catalyst with the mass loading of (B) 3 μg, (C) 3.5 μg, and (D) 6 μg; the measurements are tested in O₂-saturated 0.1M HClO₄ electrolyte. Mass activities for Pt₃Ni/C catalysts at the potential of (E) 0.9 V and (F) 0.95 V versus RHE. The dash line means the fair value.

6 μg$_{Pt}$ displayed a high ~72% inaccuracy and deviation, which also indicated the importance of the suitable mass loading of catalyst and choice of potential to study the ORR activity (Figure 4E). We also compared the ORR activity at 0.95V for both the two RDEs (red line in Figures 5B and 5F), where the potential was located in the applicable Tafel slope region for both of them. It can be found that the activity results based on the K-L method were much similar and showed a reasonable deviation between each other. This also indicated that in the reasonable potential windows range, different Pt loadings would not lead to unfair evaluation of ORR. All the earlier discussions unambiguously proved the importance of a suitable choice of loading and potential to reveal the intrinsic activity of the ORR catalyst.

It also must be considered that the structure of catalysts would have a significant influence on ORR performance. Hence, nowadays, most of the advanced electrocatalyst studies focused on the influence of kinds of structures (structure/property relationships) but may ignore the rationality when processing the analyzation based on RDE test. Furthermore, as mentioned earlier, a rational mass loading or potential choice is very critical to compare the ORR performances and indicate their intrinsic catalytic ability.
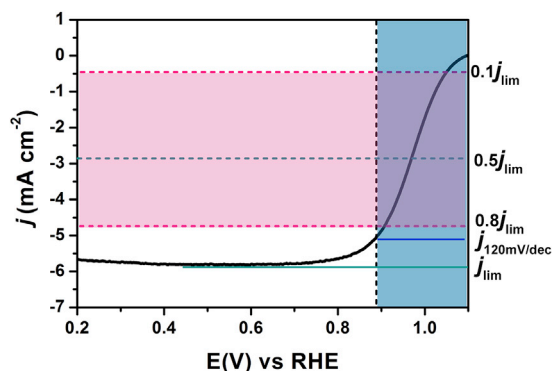
Figure 5. The Recommended Potential or Current Regions for the Minimized Relative Error, Accurate Evaluation, and Comparison of ORR Activities Based on the K-L Equation Method

The pink color region was suggested to calculate the activity in the current region of $0.1j_{lim} < j < 0.8j_{lim}$. The light blue region means the region based on the Tafel plot point< 120 mV/dec, which guarantees the reaction limited by the initial reduction of O_2, and the real intrinsic ORR activity of catalysts. j_{lim} means the limited diffusion of current density, and $0.5j_{lim}$ means the half-wave potential current.

Hence, to realize the purpose of accurate ORR evaluation, it suggests the importance of the rational benchmarking of ORR. In conclusion, we propose here the following guidelines to reasonably compare the ORR activity of catalysts:

i)   To form a uniform and full film in the RDE, the loading of catalyst should not be too low; the mass loading also should not be too high, because too high loading of catalyst would suppress the O_2 mass transportation (Higuchi et al., 2005; Xiong et al., 2018; Suntivich et al., 2010). Too high loading will introduce an extremely thick film layer on the RDE. Such a thick layer would make the O_2 mass transportation very difficult for the interior layer catalysts. In addition, the RDE theory is that based on the diffusion-convection kinetics of the pure solution laminar flow, the too thick layer would block the interior catalysts to behave in such a way. A thinner catalyst layer could help to promote O_2 diffusion in the ORR process while maintaining the high intrinsic electrocatalytic activity, whereas a too thick layer would increase the mass transport resistance for the ORR.

ii) For the Pt catalyst, the limited-diffusion current must reach the theoretical value ($\sim$5.5 mA/cm^2, within a variation of 10%).

iii) The potential chosen to process the kinetic current needs to be at the region <120 mV/dec to guarantee the reasonable accuracy and minimized relative error when evaluating the activity (Figure 5). In this regard, if one must compare the performance in specific potential, one can adjust the catalyst's mass loading to make the specific potential locate in the kinetic-controlled region. There are also some reports that claimed the current at the potential of interest has to be within 10% and 80% of the limited-diffusion current (Figure 5) (Mayrhofer et al., 2008), which has actually the similar purpose as our description. Our proposal provides a guide method by using the Tafel plot to rationalize the accurate evaluation of ORR. In practical evaluation, the chosen ideal potential should be below the half-wave potential. Too small current density will also induce magnification of errors, which also should be avoided ($>0.1j_{lim}$).

CONCLUSION

In summary, we discussed the influence in the ORR evaluation accuracy of the catalyst mass loading on RDE and the choice of potential to study the activity in ORR. Using unsuitable potential approaching the limited-diffusion current can boost the ORR activity to extremely high values, which makes it not appropriate to compare with other materials. Henceforth, it is more practically meaningful to compare the activity in a kinetic-control region or adjust the potential (0.9 V) to such a region by tuning the mass loading. To compare the performance of different catalysts, the guidelines for intrinsic activity are recommended. The perspective provided in this study could further enable more approaches to accurately evaluate and benchmark the intrinsic activity of the high-performance ORR catalysts and further the field considering RDE evaluation of next-generation catalysts.

Limitations of Study

In this study, we systemically studied the accuracies when carried out the ORR performance of typical catalysts of Pt and Pt$_3$Ni nanoparticles and gives some guidelines to rationally compare and benchmark the

performance by combining the practical study and Tafel plots. However, the exact mechanism, reason, and discussion on why only some potentials region is rational and how could the RDE performances reflect the catalysts' MEA performance is still needed to be further explored.

Resource Availability

Lead Contact

Further information and requests for resources and reagents should be directed to and will be fulfilled by the Lead Contact, Jianbo Wu (jianbowu@sjtu.edu.cn).

Materials Availability

This study did not generate new unique reagents.

Data and Code Availability

This study did not generate/analyze datasets/code.

METHODS

All methods can be found in the accompanying Transparent Methods supplemental file.

SUPPLEMENTAL INFORMATION

Supplemental Information can be found online at https://doi.org/10.1016/j.isci.2020.101532.

AUTHOR CONTRIBUTIONS

W. C. and Q. X. contributed equally to this work. W. C. and Q. X. conceived the idea and analyzed the results. W. C. and Q. X. assisted the electro-measurement and data analysis. W. C., Q. X., and J. W. wrote the paper with the assistance of all the authors. W. S., P. T, and C. S. also helped to discuss the manuscript. T. D. gave the support and also helped to revise the paper. J.W. oversaw the project. All authors discussed the results and contributed to the manuscript.

DECLARATION OF INTERESTS

The authors declare no competing interests.

REFERENCES

Blizanac, B.B., Ross, P.N., and Marković, N.M. (2006). Oxygen reduction on silver low-index single-crystal surfaces in alkaline Solution: rotating ring DiskAg(hkl) studies. J. Phys. Chem. B 110, 4735–4741.

Bu, L.Z., Zhang, N., Guo, S.J., Zhang, X., Li, J., Yao, J.L., Wu, T., Lu, G., Ma, J.Y., Su, D., and Huang, X.Q. (2016). Biaxially strained PtPb/Pt core/shell nanoplate boosts oxygen reduction catalysis. Science 354, 1410–1414.

Chen, C., Kang, Y.J., Huo, Z.Y., Zhu, Z.W., Huang, W.Y., Xin, H.L.L., Snyder, J.D., Li, D.G., Herron, J.A., Mavrikakis, M., et al. (2014). Highly crystalline multimetallic nanoframes with three-dimensional electrocatalytic surfaces. Science 343, 1339–1343.

Damjanovic, A., and Sepa, D.B. (1990). An analysis of the pH dependence of enthalpies and Gibbs energies of activation for $_2$ reduction at Pt

electrodes in acid solutions. Electrochim. Acta 35, 1157–1162.

Gasteiger, H.A., Kocha, S.S., Sompalli, B., and Wagner, F.T. (2005). Activity benchmarks and requirements for Pt, Pt-alloy, and non-Pt oxygen reduction catalysts for PEMFCs. Appl. Catal. B-Environ. 56, 9–35.

Higuchi, E., Uchida, H., and Watanabe, M. (2005). Effect of loading level in platinum-dispersed carbon black electrocatalysts on oxygen reduction activity evaluated by rotating disk electrode. J. Electroanal. Chem. 583, 69–76.

Holewinski, A., and Linic, S. (2012). Elementary mechanisms in electrocatalysis: revisiting the ORR Tafel slope. J. Electrochem. Soc. 159, 864–870.

Huang, X.Q., Zhao, Z.P., Cao, L., Chen, Y., Zhu, E.B., Lin, Z.Y., Li, M.F., Yan, A.M., Zettl, A., Wang, Y.M., et al. (2015). High-performance transition metal-doped Pt3Ni octahedra for oxygen reduction reaction. Science 348, 1230–1234.

Li, J.R., Sharma, S., Liu, X.M., Pan, Y.T., Spendelow, J.S., Chi, M.F., Jia, Y.K., Zhang, P., Cullen, D.A., Xi, Z., et al. (2019). Hard-magnet L1(0)-CoPt nanoparticles advance fuel cell catalysis. Joule 3, 124–135.

Li, M.F., Zhao, Z.P., Cheng, T., Fortunelli, A., Chen, C.Y., Yu, R., Zhang, Q.H., Gu, L., Merinov, B.V., Lin, Z.Y., et al. (2016). Ultrafine jagged platinum nanowires enable ultrahigh mass activity for the oxygen reduction reaction. Science 354, 1414–1419.

Liu, M.L., Zhao, Z.P., Duan, X.F., and Huang, Y. (2019). Nanoscale structure design for high-

performance Pt-based ORR catalysts. Adv. Mater. *31*, e1802234.

Marković, N.M., Gasteiger, H.A., Grgur, B.N., and Ross, P.N. (1999). Oxygen reduction reaction on Pt(111): effects of bromide. J. Electroanal. Chem. *467*, 157–163.

Marković, N.M., Schmidt, T.J., Stamenković, V., and Ross, P.N. (2001). Oxygen reduction reaction on Pt and Pt bimetallic surfaces: a selective review. Fuel Cells *1*, 105–116.

Mayrhofer, K.J.J., Strmcnik, D., Blizanac, B.B., Stamenkovic, V., Arenz, M., and Markovic, N.M. (2008). Measurement of oxygen reduction activities via the rotating disc electrode method: from Pt model surfaces to carbon-supported high surface area catalysts. Electrochim. Acta *53*, 3181–3188.

Pasti, I.A., Gavrilov, N.M., and Mentus, S.V. (2012). Potentiodynamic investigation of oxygen reduction reaction on polycrystalline platinum surface in acidic solutions: the effect of the polarization rate on the kinetic parameters. Int. J. Electrochem. Soc. *7*, 11076–11090.

Pedersen, C.M., Escudero-Escribano, M., Velazquez-Palenzuela, A., Christensen, L.H., Chorkendorff, I., and Stephens, I.E.L. (2015). Benchmarking Pt-based electrocatalysts for low temperature fuel cell reactions with the rotating disk electrode: oxygen reduction and hydrogen

oxidation in the presence of CO (review article). Electrochim. Acta *179*, 647–657.

Shao, M.H., Chang, Q.W., Dodelet, J.P., and Chenitz, R. (2016). Recent advances in electrocatalysts for oxygen reduction reaction. Chem. Rev. *116*, 3594–3657.

Stephens, I.E.L., Rossmeisl, J., and Chorkendorff, I. (2016). Toward sustainable fuel cells. Science *354*, 1378–1379.

Suntivich, J., Gasteiger, H.A., Yabuuchi, N., and Shao-Horn, Y. (2010). Electrocatalytic measurement methodology of oxide catalysts using a thin-film rotating disk electrode. J. Electrochem. Soc. *157*, 1263–1268.

Tian, X.L., Zhao, X., Su, Y.Q., Wang, L.J., Wang, H.M., Dang, D., Chi, B., Liu, H.F., Hensen, E.J.M., Lou, X.W., and Xia, B.Y. (2019). Engineering bunched Pt-Ni alloy nanocages for efficient oxygen reduction in practical fuel cells. Science *366*, 850–856.

Walsh, D.A., Ejigu, A., Smith, J., and Licence, P. (2013). Kinetics and mechanism of oxygen reduction in a protic ionic liquid. Phys. Chem. Chem. Phys. *15*, 7548–7554.

Wang, J.X., Junliang Zhang, A., and Adzic, R.R. (2007). Double-trap kinetic equation for the oxygen reduction reaction on Pt(111) in acidic media. J. Phys. Chem. A *111*, 12702–12710.

Wu, J., Gross, A., and Yang, H. (2011). Shape and composition-controlled platinum alloy nanocrystals using carbon monoxide as reducing agent. Nano Lett. *11*, 798–802.

Wu, J.B., Qi, L., You, H.J., Gross, A., Li, J., and Yang, H. (2012). Icosahedral platinum alloy nanocrystals with enhanced electrocatalytic activities. J. Am. Chem. Soc. *134*, 11880–11883.

Wu, J., and Yang, H. (2013). Platinum-based oxygen reduction catalysts. Accounts of Chemical Research *46*, 1848–1857 In press.

Wu, J.B., Zhang, J.L., Peng, Z.M., Yang, S.C., Wagner, F.T., and Yang, H. (2010). Truncated octahedral Pt_3Ni oxygen reduction reaction electrocatalysts. J. Am. Chem. Soc. *132*, 4984–4985.

Xiong, Y., Xiao, L., Yang, Y., Disalvo, F.J., and Abruna, H.D. (2018). High-loading intermetallic Pt_3Co/C core-shell nanoparticles as enhanced activity electrocatalysts toward the oxygen reduction reaction (ORR). Chem. Mater. *30*, 1532–1539.

Zhou, R., Zheng, Y., Jaroniec, M., and Qiao, S.Z. (2016). Determination of electron transfer umber for oxygen reduction reaction: from theory to experiment. ACS Catal. *6*, 4720–4728.

Supplemental Information

Reconsidering the Benchmarking Evaluation of Catalytic Activity in Oxygen Reduction Reaction

Wenlong Chen, Qian Xiang, Tao Peng, Chengyi Song, Wen Shang, Tao Deng, and Jianbo Wu

Transparent Methods

Chemicals and Materials:

Commercial Pt/C (Platinum, nominally 20% on carbon black) was purchased from Alfa Aesar and the Perchloric acid (HClO₄, 99.999% trace metals basis) was purchased from Aldrich. Nafion perfluorinated resin solution (Sigma Aldrich, 5 wt%) was purchased from Sigma Aldrich. Platinum(II) acetylacetonate (Pt(acac)$_2$, Strem Chemical), nickel(II) acetylacetonate (Ni(acac)$_2$, Strem Chemical), oleylamine (OAm, Sigma Aldrich), oleic acid (OA, Sigma Aldrich), benzyl ether (BE, Sigma Aldrich), tungsten hexacarbonyl (W(CO)$_6$, Strem Chemical) were all used as received. Oxygen (O$_2$, 99.999%) and argon (Ar, 99.999%) were purchased from Shanghai Weichuang Standard Gas Analytical Technology Co., Ltd. All chemicals used in this study were used without further purification. The deionized water (18.2 MΩ·cm) used in all experiments was prepared by using a Milli-Q ultra-pure purification system.

Synthesis of Pt₃Ni:

For the typical synthesis of Pt₃Ni, a modified method was used referred to the previous report (Choi et al., 2013). 0.102 mmol of Pt(acac)$_2$ and 0.08 mmol Ni(acac)$_2$ were added to the mixture of 4.0 mL OAm, 2.0 mL OA and 14.0 mL BE, and after then this mixture was heated to 130 °C under Ar with continuously magnetic stirring. Then 0.28 mmol W(CO)$_6$ was

quickly added to the heated mixture. Subsequently, this mixture was then heated to 230 °C and kept for 30 min. After the reaction, the room temperature reaction mixture with the Pt_3Ni octahedra was precipitated out by sequentially adding toluene and ethanol. The supernatant was removed by centrifugation at 8,000 rpm for 10 min for 5 times.

Electrochemical Measurements:

All electrochemical measurements were characterized on an electrochemical work station (CHI760E, CHI instrument, and SP-200, Bio-Logic) in a three-electrode configuration. The reference electrode was while a Pt wire was used as the counter electrode. The glassy carbon rotating disk electrode (RDE) with an area of 0.196 cm_2 was performed as working electrode which connected to the installation of rotating electrode speed control. Prior to the test measurements, the purchased RHE electrode was already corrected before all the measurements. All the potentials reported in our manuscript were referenced to RHE.

Preparation of RDE film. The GC electrode was polished with Al_2O_3 powder, washed with ethanol and deionized water, and dried before use. 5 mg metal/carbon (Pt/C, or Pt_3Ni: Carbon= 1:4) catalysts and 25 μl of Nafion solution (5 wt%) were dispersed in 5 ml of water-isopropanol solution with a volume ratio of 4:1 by sonicating for 10 min to form a homogeneous ink. Then the Pt concentration was measured by ICP, to

ensure the accuracy of the Pt loading. To obtain different desired catalysts mass loading on the RDEs, the corresponding calculated amount volume of the above ink was dropped onto the RDE for the Pt/C or Pt$_3$Ni/C, respectively, using a pipette and dried in air. Before the electrochemical test, the RDE film surface was wetted by DI water.

The CV measurements were conducted in an Ar saturated 0.1 M HClO$_4$ solution at room-temperature from 0.05 V to 1.1 V vs. RHE with a scan rate of 50 mV/s. The ORR activity was tested in an O$_2$ saturated 0.1 M HClO$_4$ electrolyte and maintained the O$_2$ bubble during the whole measurement. The linear scan rate was set to 10 mV/s from 0 V to 1.1 V vs. RHE in the positive direction at a rotation rate of 1600 rpm.

The ORR activity was obtained after the iR correction to the LSV. Typically, the iR correction is according to the following equation,

$E=E_{RHE}-i$R,

where E is the potential after iR-corrected, E_{RHE} is the measured potential referred to RHE, i represents the measured current, and R is the uncompensated resistance which could be determined by electrochemical impedance spectra (EIS). The typical EIS test for resistance evaluation is conducted by measuring the ac impedance spectra from 100 kHz to 0.1 Hz with a voltage perturbation of 10 mV vs open-circuit potential. The uncompensated resistance is found as the impedance where the imaginary part of the impedance is zero in a Nyquist plot.

In order to quantitatively evaluate the ORR activity for different Pt catalysts, the kinetic currents of the ORR polarization curves were calculated by the following Koutecky-Levich equation (Shao et al., 2016).

$$i_k = \frac{1}{1/i - 1/i_{lim}}$$

where i is the measured current density from the LSV curves and i_k is the kinetic current density to evaluate the activity. Then i_k can then be normalized against Pt mass to obtain the mass activities (i_{mass}), respectively (Bard and Faulkner, 2000).

Tafel plots were obtained from the LSV of different catalysts at 1600 rpm with a scan rate of 10 mV/s in O_2 saturated 0.1M $HClO_4$.

Reference

Bard, A. J. & Faulkner, L. R. 2000. *Electrochemical Methods: Fundamentals and Applications*, Wiley.

Choi, S. I., Xie, S. F., Shao, M. H., Odell, J. H., Lu, N., Peng, H. C., Protsailo, L., Guerrero, S., Park, J. H., Xia, X. H., Wang, J. G., Kim, M. J. & Xia, Y. N. (2013). Synthesis and Characterization of 9 nm Pt-Ni Octahedra with a Record High Activity of 3.3 A/mg$_{(Pt)}$ for the Oxygen Reduction Reaction. Nano Lett. *, 13*, 3420-3425.

Shao, M., Chang, Q., Dodelet, J.P. & Chenitz, R. (2016). Recent Advances in Electrocatalysts for Oxygen Reduction Reaction. Chemical Reviews*, 116*, 3594-3657.